JBC Papers in Press. Published on June 6, 2011 as Manuscript M111.254383
The latest version is at http://www.jbc.org/cgi/doi/10.1074/jbc.M111.254383

Identification of a Replication-Independent Replacement Histone H3 in the Basidiomycete *Ustilago maydis**

Verma, Anju, Tamas Kapros, and Jakob H. Waterborg
From Division of Cell Biology and Biophysics, School of Biological Sciences, University of Missouri-Kansas City, Kansas City, Missouri 64110
Running head: Replacement Histone H3 in *Ustilago*
Address correspondence to: Jakob H. Waterborg, Ph.D., UMKC, 414 BSB, 5007 Rockhill Road, Kansas City, MO 64110-2499. Tel: (816) 235-2591; Fax: (816) 235-1503; Email: WaterborgJ@umkc.edu

***Ustilago maydis* is a haploid basidiomycete with single genes for two distinct histone H3 variants. The solitary U1 gene codes for H3.1, predicted to be a replication independent (RI) replacement histone. The U2 gene is paired with histone H4 and produces a putative replication coupled (RC) H3.2 variant. These predictions were evaluated experimentally. U2 was confirmed to be highly expressed in S phase, had reduced expression in hydroxyurea, and H3.2 protein was not incorporated into transcribed chromatin of stationary phase cells. Constitutive expression of U1 during growth produced ~25% of H3 as H3.1 protein, more highly acetylated than H3.2. The level of H3.1 increased when cell proliferation slowed, a hallmark of replacement histones. Half of new H3.1 incorporated into highly acetylated chromatin was lost with a half-life of 2.5 hrs, the fastest rate of replacement H3 turnover reported to date. This response reflects the characteristic incorporation of replacement H3 into transcribed chromatin, subject to continued nucleosome displacement and loss of H3 as in animals and plants. While the two H3 variants are functionally distinct, neither appears to be essential for vegetative growth. Knockout (KO) gene disruption transformants of the U1 and U2 loci produced viable cell lines. The structural and functional similarities of the Ustilago RC and RI H3 variants with those in animals, in plants and in ciliates are remarkable because these distinct histone H3 pairs of variants arose independently in each of these clades and in basidiomycetes.**

Core histones provide the packaging proteins for DNA in eukaryotic cells. During S phase when genomic DNA is duplicated, replication coupled expression of histone genes provides new protein to assemble newly replicated DNA. Histone chaperones assist in the creation of new nucleosomes in order to maintain a stable, compacted, repressed state of chromatin. Within this context, regulatory proteins modulate chromatin environments to facilitate access to the DNA for gene transcription. The components and processes that allow RNA polymerases to transcribe a chromatin template, such as epigenetic modifications of DNA and histones, are being identified and intensely studied. The processes of nucleosome displacement from DNA by transcribing RNA polymerases and of nucleosome re-assembly from available histones remain poorly understood.

In research going back decades, it was observed that the composition of nucleosomes across transcribed gene regions, identified in part by high levels of histone acetylation, changed over time. Replication-coupled (RC) histone H3 variants like H3.2 in birds were replaced by histone H3.3, a constitutively expressed form of animal histone H3. This histone is now known as a replacement histone or as a replication-independent (RI) H3 variant (1,2). Specialized chaperones such as HIRA and Daxx selectively bind these RI H3 proteins at a small region, residues 87-90, which is uniquely different between RI and RC forms (3,4). In S phase RC and RI variants are both present for replication associated chaperones to assemble nucleosomes. Outside of S phase transcribed genes are only repackaged using new RI H3 proteins. The basis for this selectivity is found in one or more of the following reasons: outside of S phase RC H3 proteins are not synthesized; histone H3 molecules from displaced nucleosomes cannot be re-used in nucleosome assembly; and transcription associated chaperones like HIRA use only RI H3 sequence variants.

Many of these processes have been identified and studied in *Saccharomyces cerevisiae* as a simple model system. However, this yeast makes only a single H3 protein from 2 histone H3 genes. This H3 is produced in a replication coupled pattern of expression with significant H3 protein availability outside of S phase. It acts like an animal H3.3 in that it is used by HIRA (4). In *Schizosaccharomyces pombe*, a single H3 protein is produced, partly from 2 RC H3 genes and partly from 2 constitutive ones (5). Neither model organism can be used to study the contribution of histone H3 variants in replicative and replacement nucleosome assembly.

Study of the functions provided by RC and RI H3 variants in animals and in plants is limited because the multiplicity of genes of both types prevents effective use of gene knockout and replacement approaches. In each case, the duplication of the ancestral histone H3 and the structural and functional differentiation into replicative RC and replacement RI H3 variants arose independently (6-8). Gorovsky and coworkers have used the diploid protist *Tetrahymena* as a model system. In ciliates, distinct RC and RI H3 genes have arisen independently from their appearance in animals and in plants (6-8). In Tetrahymena with 2 RC and 2 RI loci, complete knockout of both RC or both RI loci produces viable vegetative cells. In RC knockouts, replication results in dramatically reduced cell proliferation rates and hypoploidy, likely due to insufficient nucleosome formation using only RI H3 histone. Proficient growth required upregulation of RI loci. Conversely, RI knockouts are viable but fail to produce viable spores (9). The validity of these results for animals or plants has not been confirmed. The sequence differences between the RC and RI H3 variants in Tetrahymena involve many more residues than the distinctive 3-5 that exist between animal and plant H3 variants.

Ahmad and Henikoff had suggested that the basidiomycete *Cryptococcus* might contain a replacement H3 variant (10). Genome sequencing of the related corn smut *Ustilago maydis* revealed that this haploid organism has two distinct H3 genes. One is paired with the single histone H4 gene, an organization often seen for RC histones, and the other one is a solitary gene, like animal H3.3, with a replacement-like variant sequence at residues 89 and 90 (11) (Fig. 1). We have evaluated the expression and stability of the Ustilago histone H3 proteins. We have concluded that the solitary H3 gene indeed has all the functional characteristics of a replacement RI H3 variant and that the H4-paired H3 gene is an RC variant. The similarities of the Ustilago H3 variants in gene structural organization, in the differences of the polypeptides produced, in the selectivity of incorporation into replicative and transcription linked nucleosomes, and in protein stability with the RC and RI H3 variants in plants and in animals is remarkable. It provides insight in the conserved nature of nucleosome assembly processes because the RC-RI H3 divergences arose hundreds of millions of years apart, each time at the ancestral root of what have become broad clades of diverse, multicellular eukaryotes (6).

We have begun to exploit the possibilities for homologous gene replacement in *U. maydis* (12) and complementation by plasmid-based histone H3 mutants to evaluate the contribution of these two H3 variants in nucleosome assembly during transcription and replication. The viability of strains with knocked out (KO) U1 or U2 loci, coding for the RI H3.1 and RC H3.2 variants, respectively, is reported.

Experimental Procedures

Culture of Ustilago. *Ustilago maydis* 521, strain 9021 obtained from the Fungal Genetics Stock Center (UMKC, Kansas City, MO) and defined as wild-type (wt), was grown in Synthetic Dextrose (SD) medium (6.7 g Difco Yeast Nitrogen Base without amino acids (Benton-Dickinson, Sparks, MI) with 20 g glucose per Liter) at 30 °C on 2 % agar or in liquid culture at 150 rpm with typical experimental use at ~10^7 cells/ml. Cell density was determined by hematocytometer counting. Stationary phase conditions developed for wt cells above 2 x 10^7 cells/ml in SD medium. Labeling *in vivo* with [^{3}H] acetic acid (20 Ci/mmol; MP Biomedicals, Irvine, CA) was performed at 4 mCi/L for 5 min, unless specified otherwise, after 10 min preincubation at 10 µg/ml cycloheximide (Sigma, St.Louis, MO), added from 2 mg/ml stock in ethanol. Labeling with [4,5-^{3}H] L-lysine (60

Ci/mmol; MP Biomedicals) was performed at 0.4 mCi/L for 30 min, unless specified otherwise, and with [^{35}S] L-methionine (540 Ci/mmol; MP Biomedicals) at 0.1 mCi/L for 20 min. Cell cycle progression was arrested in S phase by the addition of 10 % (w/v) hydroxyurea to 1 mg/ml (13) in 1 L log cultures at 2.2 x 10^6 cells/ml for 90 min. Cells were released from the block by washing with preconditioned SD medium. Tritiated lysine (50 μCi) was added to each culture during the last 30 min prior to cell collection after the culture was concentrated to 250 ml by centrifugation (5 min, 800 x *g*). The distribution of cells across G1, S and G2/M phases was determined by flow cytometry as described (13) in a FACScalibur 877 (Benton-Dickinson) with ModFit LT (Verity Software) data analysis.

Purification of histone H3. Histones were extracted and purified from cell pellets essentially as described (14). Cells from 0.25 to 2.0 L culture were collected by centrifugation (5 min, 800 x *g*) and resuspended into 2 to 4 pellet volumes of 40 % GuCl in KP_i (40 % guanidine.HCl, 0.05 M KH_2PO_4, 0.05 M K_2HPO_4, adjusted by KOH to pH 6.8, with 1.4 mM 2-mercaptoethanol). Cells were sonicated on ice in aliquots of 15 ml for twice 5 min with a Branson Sonifier 400 with medium tip at 25 % initial output with cooling break which resulted in 90+ % cell breakage, clarified (10 min, 30,000 x *g*), incubated on ice for 15 min at 0.25 N HCl, clarified (30 min, 30,000 x *g*), diluted with 0.1 M KP_i pH 6.8 to the refractive index of 5 % GuGl in KPi, adjusted to 1.4 mM 2-mercaptoethanol, and incubated overnight under rocking with 1 ml settled BioRex70 resin (200-400 mesh, Bio-Rad, Richmond, CA) per extract from 2 x 10^{10} cells, an experimentally optimized ratio for the *Ustilago* procedure. After repeated washing by 1 x *g* settling of the resin from 5 % GuCl in KP_i until the supernatant was clear, resin was placed in a small column, washed with 8 volumes 5 % GuCl in KP_i and histones were eluted by 10 volumes 40 % GuCl in KP_i. Histones were dialyzed in 3,500 MW cut-off Spectra/Por 3 dialysis membranes (Spectrum Labs, Rancho Dominguez, CA) thrice against 100 volumes 2.5% acetic acid with 1.4 mM 2-mercaptoethanol, and recovered by lyophylization. Histone H3 was purified by reversed-phase hplc on Zorbax Protein-Plus columns (0.4 x 25 cm, New England Nuclear) as described (14). Crude histones were dissolved in 0.25 ml 8 M urea in 1 M acetic acid and injected in the column, equilibrated at 1 ml/min with 40 % acetonitrile (Fisher Scientific, St.Louis, MO) in 0.1 % TFA (Sigma), washed for 2 min in this solvent, and eluted by a gradient from 40 to 55 % acetonitrile in 0.1 % TFA over 45 min. The two histone H3 variants co-eluted 43 min after injection, as monitored by absorbance at 214 nm. They were identified by AUT gel electrophoresis of lyophilized column fractions based on protein size and characteristic affinity for Triton X-100 (15,16). Semi-preparative purification of histone H3 used Vydac C4 columns (214TP510, 1.0 x 25 cm, Grace, Deerfield IL) with the same elution conditions at 3 ml/min.

Polyacrylamide gel analysis. Acid Urea Triton (AUT) gel electrophoresis was performed in 15 or 30 cm long gels with Triton X-100 (Bio-Rad) at 6 mM, a concentration optimized for *Ustilago* histone H3 variant separation, as described (15,16). Proteins were quantitated by densitometry of gels, stained with Coomassie Brilliant Blue R-250 and destained in 7 % acetic acid, 20 % methanol. Specific radioactivity was determined by densitometry of fluorographic exposures exactly as described (17,18).

qRT-PCR quantitation of H3 gene transcripts. Total RNA was isolated with Trizol Reagent (Invitrogen, San Diego CA) using 0.4-0.6 mm glass beads for cell breakage for 3 min in a Mini-Beadbeater-16 (Biospec Products, Bartlesville, OK). Genomic DNA was digested with DNase I. The qRT-PCR procedure with separate cDNA synthesis step was performed according to the manufacturer's instructions using the Superscript III Platinum two-step qRT-PCR Kit with SYBR Green (Invitrogen) in an Applied Biosystems 7500 thermal cycler (Life Technologies, Carlsbad CA). *Ustilago* peptidyl-prolyl isomerase (ppi) (GenBank NW_101009, locus UM03726.1) was used as a constitutively expressed reference gene (19,20). Primers used for the amplification of histone genes (Fig. 1A) U1 (U1F and U1R), U2 (U2F and U2R) and H4 (H4F and H4R) and for the ppi gene (ppiF and ppiR) are listed in Table I. Histone mRNA qRT-PCR levels were quantitated as $2^{-\Delta Ct}$, relative to ppi levels, following manufacturer's instructions.

Transformation of Ustilago. Transformation of *U. maydis* was modified from published procedures (12,21) as follows. Cells (5 x 10^6), subcultured under continuous logarithmic growth in SD medium for at least 4 days, were collected at 10^5 cells/ml culture density by centrifugation for 5 min at 1100 x *g*, gently washed with 30 ml SCS (20 mM sodium citrate, pH 5.8, 1 M sorbitol), and resuspended in 1 ml SCS. Protoplasts were produced by adding 2 ml 128 mg/ml Vinoflow FCE (Novo, Gusmer Enterprises, Mountainside, NJ) in SCS and gentle mixing for 10 min, with microscopic verification of protoplasting. Protoplasts were collected by centrifugation for 10 min at 1100 x *g*, washed twice with 1 ml SCS, once with 1 ml STC (1 M sorbitol, 10 mM Tris.HCl pH 7.5, 100 mM $CaCl_2$) and resuspended in 1 ml ice-cold STC. A mixture of 5 µl transforming DNA at 1 mg/ml in STC and 1 µl 15 mg/ml heparin (Sigma) in STC was added to protoplasts (10^6 in 0.05 ml) on ice and incubated for 10 min. A solution of 0.5 ml 40 % (w/v) PEG-4000 (Sigma) in STC was added, incubation on ice was continued for 15 min followed by addition of 0.5 ml STC. Protoplasts were centrifuged for 5 min at 1100 x *g* and the pellet was resuspended in 0.2 ml STC. Aliquots (0.02 ml) were plated on 1 % SD agar containing 1 M sorbitol and 2 µg/ml carboxin, and grown at 30 °C. Transformants were collected after 4-5 days. Carboxin (CBX) (5,6-dihydro-2-methyl-1,4-oxathi-ine-3-carboxanilide; Vitavax) and CBX-resistance plasmid pGR3 were kind gifts from S. Gold (Athens, GA). Used without linearization as a transformation reference, pGR3 yielded thousands of transformants per plate in this procedure.

Transformation constructs. Genomic DNA was isolated by CTAB (22), as modified (23), by addition of 1 % CTAB (Sigma) in 0.1 M Tris.HCl pH 7.5, 0.7 M NaCl, 10 mM EDTA, 14 mM 2-mercaptoethanol to pelleted cells, vigorous vortexing for 3 min with 0.4-0.6 mm glass beads, incubation for 45 min at 65 °C, addition of 1 volume of chloroform:isoamyl alcohol (24:1, v/v), centrifugation for 5 min at 12,000 x *g*, DNA precipitation from the aqueous phase with 0.9 M ammonium acetate in 2-propanol and a wash of the DNA with 70 % ethanol.

For the U1 knockout (KO) construct, a 863 bp U1 left border (LB) sequence was amplified by PCR in a MJ Research PTC-225 PCR cycler (GMI, Ramsey, MN) using primer pair U1KOLBF and U1KOLBR, and a 1043 bp U1 right border (RB) sequence by primer pair U2KORBF and U2KORBR. The transformation construct was assembled by ligation of *Eco*RI and *Sac*I digested plasmid pGEM-4Z (Promega, Madison, WI) to *Sac*I and *Sfi*I digested U1 LB, the CBX cassette excised by *Sfi*I from pMF1-c (12), kindly provided by M. Feldbrügge (Düsseldorf, Germany), and the *Sfi*I and *Eco*RI digested U1 RB. The construct was linearized by *Xba*I or *Sma*I for use in transformation through double-strand DNA repair-based homologous recombination (24). The equivalent U2 KO transformation construct was ligated using *Hin*dIII and *Sal*I restricted pGEM-4Z, the *Sal*I and *Sfi*I digested 1020 bp U2 LB amplified by PCR primer pair U2KOLBF and U2KORBR, the CBX cassette excised by *Sfi*I from pMF1-c, and the *Sfi*I and *Hin*dIII digested 1015 bp U2 RB amplified by primer pair U2KORBF and U2KORBR, and linearized by *Sac*I for use in transformation. Constructs were verified by restriction digestion and sequencing.

CBX-resistant colonies were subcultured into liquid SD at 3 µg/ml carboxin. Genomic DNA was prepared and homologous recombination at the targeted U1 and U2 loci was analyzed by PCR using a variety of primer pairs which uniquely recognized sequences within the transforming constructs, the carboxin-resistance cassette, and sequences inside and beyond the border sequences. These primer sequences will be provided upon request. Two U1KO transformation experiments produced 65 CBX-resistant clones which grew in liquid SD and continued growth when selection was removed. Eight strains contained KO recombination events at the U1 locus and likely were heterokaryons. Clone 47 was identified as a homokaryon U1 knockout containing the CBX cassette with error-free homologous recombination in LB and RB sequences, as confirmed by sequencing. Multiple confirmed U2 knockout strains were obtained from recombinant heterokaryon strains which contained both wild-type and knocked out U2 loci in varying ratios, as measured by PCR analysis (data not shown). Continued culture under selection produced stable, slow growing homokaryon lines which subsequently could be

maintained without carboxin selection and which contained only the CBX-interrupted U2 locus as verified by PCR analysis and sequencing. Transformed KO lines maintain viability when stored at –80 °C in 15 % glycerol.

RESULTS

Identification of Ustilago H3 variants. Sequencing of the genome of the haploid basidiomycete *Ustilago maydis* revealed the existence of two single-copy histone H3 genes (11), one on chromosome 11 as a solitary histone, named U1 (GenBank AACP01000135.1, locus UM03916.1) and one, named U2, in a divergently transcribed gene pair with histone H4 on chromosome 6 (GenBank AACP01000090.1, locus UM02709.1) (Fig. 1A). These histone forms differ only in a few amino acids, including residues 89-90 (Fig. 1B). This region defines the replacement character of animal histone H3.3 (4,25), that interacts with the specific replication-independent histone chaperones HIRA and Daxx (3), and that exists in the independently evolved replacement H3 variants of higher plants (8,26-28) and ciliates (7). The characteristic sequence at residues 87-90 was the basis for the suggestion that the basidiomycete *Cryptococcus* might also contain this type of replacement histone H3 (10). We chose to use *U. maydis* as the model system (29) to evaluate the existence of a replacement histone H3 in basidiomycetes. We anticipated that the methionine-containing U2 gene, which shares its promoter region with the single histone H4 gene (Fig. 1), would be expressed in S phase.

BioRex70-based histone isolation from whole cells under denaturing conditions to preserve post-synthetic modifications and protein integrity was followed by reversed-phase chromatography. The co-eluting histone H3 variants were separated by AUT gel electrophoresis (Fig. 2A) and named in order of increasing gel mobility H3.1 and H3.2, based on the standard method of core histone variant nomenclature (30). [^{35}S]-methionine labeling identified U2 as the gene that codes for histone variant H3.2 (Fig. 2B) based on the single methionine in the mature protein (Fig. 1B). This indirectly identified U1 as the gene that produces histone H3.1 (Fig. 1A).

Relative abundance of H3 variants. The relative amounts of the two histone H3 variants varied with culture conditions. Continuous subculture to maintain logarithmic growth resulted in cells with up to 80 percent of histone H3 in the H3.2 form (lanes A and C in Fig. 2C, lane 0 h in Fig. 3A). When cultures were allowed to reach near stationary phase (2 x 10^7 cells/ml) the relative amount of H3.1 protein increased to more than 30 % while continued culture into full stationary phase, when cell budding ceases, cell walls thicken and cell density stabilizes, produces cultures with up to 50 % H3.1 protein (lane E in Fig. 2B, Fig. 3). Such a gradual replacement of proliferation associated protein by another form, named a replacement variant (25), which preferentially occurs across transcribed gene regions (31), was one of the first indications for the existence of replacement H3 histone variants (1,2). The changes in H3 variant abundance support the notion that H3.2 is a replication-coupled (RC) variant and H3.1 a replication-independent (RI) form.

Histone acetylation of H3 variants. Loss of nucleosomes across transcribed chromatin regions followed by the preferential use of replacement H3 variant forms to create new nucleosomes predicts that a replacement H3 form will show raised acetylation levels (26,32). H3.1 was acetylated 10-30 % higher than H3.2 under all growth conditions, as measured in stained AUT gels. H3.1 had 1.2-1.6 acetylated lysines (AcK) per molecule during logarithmic growth (lanes A and C in Fig. 2B and Fig. 2C). This level decreased in stationary phase (Fig. 3). New H3.1, visualized by lysine pulse labeling with up to 6 radioactive acetyl-lysines (*AcK) per molecule, contains 2.7 AcK per new H3.1 (lane D in Fig. 2B) and 1.3 per bulk H3.1 (lane C in Fig. 2B). This is higher than the 2.4 AcK per new H3.2 (lanes B and D in Fig. 2B) at a steady state of 1.1 AcK per bulk H3.2 (lanes A and C in Fig. 2B).

Pulse labeling with tritiated acetate for 5 min under conditions of histone synthesis inhibition by cycloheximide reveals that a subfraction of histone H3.1 (with 1.6 AcK/H3) (lanes A and C in Fig. 2C) is subject to very rapid acetylation at up to 6 sites with an average of 3.4 *AcK/H3.1 (lane B in Fig. 2C). Turnover is so rapid that labeling for 20 min results in a much reduced specific radioactivity, even without applying a chase protocol. The same situation has been observed

and analyzed in *Chlamydomonas* (17). The loss of acetate label due to turnover (lane D in Fig. 2C) is consistent with a half-life of less than 4-5 min. For histone variant H3.2, acetylation levels are lower. Pulse labeling produces 2.4 *AcK/H3.2 (lane B in Fig. 2C) in bulk H3.2 with 1.4 AcK/molecule (lanes A and C in Fig. 2C). Turnover appears a bit slower with a half-life of 5-6 min (data not shown). These rates of histone acetylation turnover are consistent with rates at which N-terminal lysines are acetylated and rapidly deacetylated in transcriptionally active chromatin of other species (33).

Histone synthesis of H3 variants. The rise in H3.2 abundance in growing cultures suggested a coupling between H3.2 synthesis and S phase when newly replicated DNA is packaged into chromatin. Conversely the rise in H3.1 abundance when cell proliferation ceases (Fig. 3A) predicts the absence of such a relationship and suggests cell-cycle independent histone synthesis. Such a constitutive pattern is typical for replacement H3 histones in animals (4), plants (34) and ciliates (9). This prediction was tested experimentally by RT-PCR analysis of U1 and U2 transcript levels and by measuring histone H3 variant protein synthesis rates in hydroxyurea-synchronized *U. maydis* cultures (13).

Early log phase cultures were treated for 90 min with 1 mg/ml hydroxyurea to arrest cells in S phase (13), released into conditioned SD medium, and histones were purified after 30 min pulse labeling for histone synthesis with tritiated lysine. Such a single block procedure produced a reasonable degree of synchrony in logarithmically growing cultures, as determined by flow cytometry across the first few hours after release from the block (Fig. 4G). A similar degree of synchrony was observed after a double hydroxyurea block protocol (data not shown).

Lysine pulse labeling showed that most label was observed across the tail of the histone H3 peak in reversed-phase hplc (Fig. 4A). At this position a late-eluting peak was seen in S phase-enriched cultures (Fig. 4A, 4D). Subsequent analysis (Fig. 5) showed that newly synthesized histone H3 of *U. maydis* elutes as a discrete entity, later than the bulk H3 form into which it is converted over time. For the experiment presented in Figure 4, both new and bulk histone H3 protein was pooled together and analyzed on AUT gel by Coomassie staining (Fig. 4B) and fluorography (Fig. 4C). The peak incorporation of label at 1 and 3 hours (Fig. 4A) was predominantly found in H3.2 (Fig. 4C). The specific radioactivity of H3.2 at the time of the second S phase (Fig. 4G) was reduced in prominence because the same amount of tritiated lysine was supplied to twice the number of cells (Fig. 4D). The replication coupled pattern of H3.2 gene expression was confirmed by qRT-PCR analysis of H3.2 U2 gene transcript levels. The H3.2 expression pattern was like that of the single *U. maydis* H4 gene (Fig. 4F). The slight rise in H3.1 synthesis, detected by labeling at the height of the first S phase after release from hydroxyurea (Fig. 4E), was not seen in H3.1 transcript levels (Fig. 4F). These results identify H3.1, as predicted, as a replication-independent H3 variant. The increased incorporation of constitutively transcribed H3.1 during S phase is likely to reflect co-incorporation with H3.2 protein by chaperones without H3 sequence specificity at a time when large amounts of newly replicated DNA are available for assembly into chromatin.

Turnover of histone H3.1 protein. Lysine incorporation into new H3 variants in asynchronously growing cultures showed that 60 % of the label was incorporated into the H3.1 variant which represented only 31 % of the total H3 protein (lane D in Fig 2B). A similar observation was made for the alfalfa RI H3 (26) and lead to the discovery that this alfalfa H3 variant was subject to protein turnover with a half-life of about 20 hours as part of the displacement of nucleosomes from transcriptionally active chromatin. This identified the plant RI H3 as a replacement histone variant (26). For the *Ustilago* system, this prediction was evaluated and experimentally confirmed for histone H3.1 as follows.

We took advantage of the novel observation that lysine pulse label was observed primarily in a peak of new H3 (nH3) which eluted 2 min after the main H3 (mH3) peak. The pulse label was shortened from 30 to 15 min and hplc sampling rates were doubled (Fig. 5A). During the chase period, the label shifted from the nH3 hplc peak with 22 ± 4 % (n=8) of the absorbance in H3 (Fig. 5A) to the mH3 peak with a half-life of

approximately 30 min (Fig. 5D). The H3 specific radioactivity in hplc fractions showed that 20% of label was lost in 2.5 hours (Fig. 5D).

Pooled m and n fractions were run in parallel on AUT gels, stained (Fig. 5B) and fluorographed (Fig. 5C), and the specific radioactivity of each variant was determined. New protein (n) for both variants matured to the main H3 peak (m) with a half-life of 30 min and appeared complete by 90-120 min (Fig. 5E-F). The specific labeling of H3.2 was stable for at least 2.5 hours (Fig. 5F). In contrast, H3.1 was clearly subject to protein turnover with a 50 % loss in 2.5 hours (Fig. 5E). In these cell cultures with a doubling rate of 1.7 hours, this is ~1.5 cell cycles. The pattern of specific radioactivity was fitted to linear decay patterns (Fig. 5D-F). Data precision was insufficient to determine whether turnover was linear or as expected exponential.

Histone H3 synthesis under non-proliferative conditions. Log cultures were treated for 90 min with hydroxyurea as before (Fig. 4) to stop cell proliferation. Cells were labeled for 30 min in fresh SD medium with tritiated lysine and a pulse labeled aliquot was collected. To other aliquots, hydroxyurea was added to 1 mg/ml to block cell cycle progression for an additional 2, 4, 6 or 10 hours. Culture density was monitored during this chase period and cell numbers remained unchanged. The specific labeling of H3.1 and H3.2 variants was determined by densitometry of stained and fluorographed AUT gels. The specific radioactivity of H3.2 remained unchanged throughout the experiment. The labeling of H3.1 decayed exponentially with a half-life of 3.5 to 4 hours (data not shown). This result confirmed that new H3.1 is subject to extensive turnover both in cycling and non-cycling cells.

The replication-independent pattern of H3.1 was confirmed by measuring H3.1 synthesis when hydroxyurea inhibited DNA replication (HU lanes in Fig. 6AB) and in stationary cultures when cell proliferation had ceased (Stat lanes in Fig. 6AB and 6E). In hydroxyurea, labeling of new H3.1 and H3.2 was reduced 5-10 fold (in HU lanes of Fig. 6B 14% and 22%, respectively) relative to growing cells (Log lanes in Fig. 6B). In stationary cultures, labeling of RI H3.1 was little affected (compare Stat-n and HU-n lanes in Fig. 6B). In contrast, labeling of new H3.2 dropped to less than 1% (compare Stat-n and Log-n lanes in Fig. 6B). The reduction of H3.1 labeling in non-proliferative cultures is likely to reflect loss of replicative nucleosome assembly sites while transcription linked sites persisted. In contrast, reduction of replication reduces and cessation of cell proliferation eliminates the replication-coupled synthesis and deposition of H3.2.

Taken together, these experiments demonstrate that H3.1 is a constitutively expressed, and thus replication-independent (RI), histone H3 with all functional characteristics that are seen in animal RI H3.3 and the equivalent plant replacement H3 variants. In contrast, the prominent pattern of S phase enhanced expression of H3.2, which was as strongly replication coupled as the histone H4 gene, and cessation of its synthesis when cell proliferation ceases, clearly identifies H3.2 as a replication-coupled variant.

Are RC and RI H3 variants required? The genome of haploid *U. maydis* contains single RI H3.1 (U1) gene and a single RC H3.2 (U2) gene, coupled through a shared promoter with the single H4 gene (Fig. 1A, 4F). This represents a uniquely simple system to evaluate whether either H3 variant is essential. Transformation cassettes for homologous recombination at U1 and U2 loci were created based on the knockout plasmid pMF1-c with carboxin (CBX) as selectable marker (12). Homologous recombination target sequences (~ 1 kb) were produced by PCR. The left border (LB) sequences were upstream of the TATA promoter sites of the U1 and U2 genes. The right border (RB) sequences were downstream of the end of the 3' UTRs of the U1 and U2 genes, as determined from available Genbank EST clones. A low number of stable, PCR and sequencing verified U1 knockout (U1KO) and U2 knockout (U2KO) homokaryon transformants were obtained (see Experimental Procedures). H3 proteins from U2KO and U1KO isolates on AUT gels showed the absence of H3.2 and of H3.1 protein in these strains, respectively (Fig. 6C). This showed that neither knockout causes lethality and that vegetative growth is possible with either H3 variant protein. A similar conclusion was reached in *Tetrahymena* (9). Synthesis and acetylation of H3.1 in U2KO and of H3.2 in U1KO cells in

growing and stationary cultures was indistinguishable from wt results (Fig. 6D).

Some mutant phenotypes are described below. A full phenotypic analysis of U1KO and U2KO strains will be presented elsewhere. Growth rate comparisons of wild type (wt) cells (Fig. 6E), U1KO cells (Fig. 6F) and U2KO cells (Fig. 6G) revealed that cell cycles had lengthened in the KO strains (Fig. 6H). The effect was moderate, with a 25% increase in cell doubling time for the U1KO strains without RI H3.1 protein. U1KO cells were a bit smaller than wt ones with normal budding. Histone H3 protein yield was unaffected on a per cell basis in log and stationary cultures, leading to a high protein load per AUT lane when histones were extracted from the same number of U1KO and wt cells (Fig. 6C). U1KO cultures reached stationary phase at cell densities (2 to 3 x 10^7 cells/ml) similar to wt cells (compare Fig. 6F with Fig. 6E) with wt-like changes in cell wall morphologies.

U2KO cells without RC H3.2 grew more slowly, as measured during continuous logarithmic growth, achieved by repeated dilution of cultures (Fig. 6G) with cell doubling in 4.8 hours, more than twice that of wt cells (Fig. 6H). U2KO cells were quite a bit larger than wt ones. In liquid culture, cell lengthening with septa formation and branching was observed. This mycelial-like growth was strongly enhanced in surface cultures on SD agar. Histone H3 yield on a per cell basis was increased over wt (Fig. 6C), consistent with the observation of multiple nuclei in mycelial-like cells (data not shown). Consistent with the larger cell size, U2KO cultures reached stationary culture conditions at approximately 10^7 cells/ml (Fig. 6G), 2 to 4 times lower than wt (Fig. 6E) and U1KO strains (Fig. 6F).

DISCUSSION

It is remarkable how similar the Ustilago histone H3 variants are to those in animals and in plants. Every prediction made for Ustilago, based on the established characteristics of RI and RC H3 variants in plants and in animals, was confirmed. Evolutionary analysis has demonstrated that the structural duplication and functional divergence of RI and RC variants arose independently, hundreds of millions of years apart, in those ancestral species that gave rise to the clades of animals, plants, ciliates and basidiomycetes (6). The RC and RI H3 variants arose 400 My ago in the ancestral species of all multicellular metazoa. For plants this event occurred likely more than 800 My ago. A similar H3 duplication and functional specialization occurred independently in the ciliate ancestor (7). In each case, replication coupled H3 genes persisted, in general, linked to histone H4 genes, as seen for the U2 gene in Ustilago. These genes consistently lost the ability to interact with transcription linked nucleosome assembly factors like the HIRA chaperonin due to primary protein sequence changes limited to residues 87-90 (4). The ancestral H3 form, capable of transcriptional and replicational nucleosome assembly, as demonstrated for Ustilago U1, became an unlinked gene, no longer coupled to S phase regulated histone gene clusters, with a replication independent and typically constitutive pattern of expression. In this RI H3 variant the protein sequence 87-90 that allows participation in both replicative and transcriptional chromatin formation remained invariant as demonstrated by a Tree-Of-Life evolutionary analysis (6). This characteristic results in the transcription induced displacement and linked turnover of replacement H3 variants, as demonstrated for plants (26) and now for Ustilago histone H3.1 (Fig. 5E).

Thus, the identification and characterization of the RI and RC H3 variants in Ustilago does not reveal any new ways in which these histone variants may regulate gene expression. Rather, it illustrates how conserved the nucleosome assembly processes are across the full spectrum of eukaryotic evolution. Two distinct processes arose when early eukaryotes started packaging their DNA in nucleosomes and these have continued to coexist: the addition of new nucleosomes on newly replicated DNA and the formation of replacement nucleosomes across transcribed genes in chromatin. We can only speculate that it is the increased complexity of multicellular animals, plants and basidiomycetes that made it advantageous to duplicate H3 genes and to regulate independently the production of distinct functional H3 variant proteins.

Ustilago may be a suitable model system in which the basis of this advantage can be studied. Experimentally it offers many of the opportunities of the *S. cerevisiae* for genetic analysis and

molecular manipulation that have made budding yeast such a powerful tool for the study of eukaryotic cells (11,12,29,35-37). As shown here, it has single RC and RI H3 genes which look and behave in all aspects like the analogous genes in animals and plants. In addition, the Ustilago genome has single genes for each of the essential histone types. Histone H4 (102 amino acids) (Genbank UM02710.1) is divergently transcribed from the 135 residue H3.2 gene U2 to which it is linked (Fig. 1A). In addition to the unlinked H3.1 gene U1, Ustilago contains a single centromeric cenH3 (139 residues) on chromosome 19 (locus UM05257.1) and H2A.Z (134 residues) on chromosome 1 (locus UM01504.1). The H2A (135 residues) and H2B (141 residues) genes are paired on chromosome 3 (locus UM01504.1-UM01505.1). The similarities in histone polypeptide size (range 134-141, except for H4) prevent analysis of total histone extracts by SDS gel electrophoresis. We used the combination of reversed-phase hplc fractionation and AUT gel electrophoresis to study the histone H3.1 and H3.2 protein variants.

Histone H3 acetylation. Acetylation levels of the Ustilago histone H3 variants – 10-30 % higher in the RI H3.1 protein than in H3.2 histone – ranged between 0.9 and 1.7 acetylated lysine per polypeptide chain, depending on culture conditions. This is slightly lower than the steady state levels of 1.8-2.1 in *S. cerevisiae* (38). Lysine labeling revealed much higher levels of acetylation in newly synthesized H3 for H3.1 with 3.1 ± 0.4 (n=5) and for H3.2 with 2.7 ± 0.3 (n=5) acetylated lysines (Fig. 5). In each case, non-acetylated forms did not exist immediately following histone synthesis. This suggested that each new H3 polypeptide was quantitatively acetylated at one particular lysine. The level and pattern of acetylation in AUT fluorographs (Fig. 2B, 4, 5) suggests that, in addition, N-terminal lysines 9, 14, 18, 23 and 27 are acetylated to a higher extent in new H3 than in bulk H3 protein. In yeasts high levels of acetylation of lysine 56 have been reported (39,40). Histone acetyltransferase Rtt109 is thought to be responsible for the transient complete acetylation of H3K56 during nucleosome assembly in replicative chromatin, during DNA repair or associated with transcription (40-47). Support for the involvement of H3K56 acetylation comes from the increased acetylation of new H3.2 protein under conditions of replicative stress induced by hydroxyurea (lane HU-n in Fig. 6B), as reported for *S. cerevisiae* (41). Study of the sites and extent of lysine acetylation in new and matured H3 proteins of *U. maydis* and *S. cerevisiae*, separated by reversed-phase hplc, is in progress and will be reported elsewhere.

Are both histone H3 variants of Ustilago essential? The multiplicity of RC and RI H3 genes in animals and plants prevents one from addressing experimentally, by gene knockout, the simple but important question: "Can the cell live with just one of the functionally distinct histone H3 variant forms?" Full knockout analysis for the two RC and two RI H3 genes of diploid Tetrahymena has been reported (9). Remarkably, neither H3 variant appeared essential under vegetative growth conditions. However, reduced availability of new H3 protein caused reduction in growth rates while, for as yet unresolved reasons, the RI H3 variant appears to be required to produce viable sexual progeny (9).

In haploid Ustilago, gene disruption of the single U1 and U2 loci is relatively efficient. Following curing of the initial heterokaryons, which grew like wt cells, by continued subculture under selection, viable and stable U1KO and U2KO homokaryon strains were isolated that did not produce any histone H3.1 or H3.2 protein, respectively (Fig. 6C). Synthesis and acetylation of the single H3 variant appeared unaffected. In U1KO cells the amount of H3.2 protein per cell was approximately the same as the combined amount of H3.1 and H3.2 protein per wt cell (Fig. 6C). The cell doubling time increased by ~25% (Fig. 6H), consistent with the ~25% steady state level of H3.1 protein (Fig. 2B, Fig. 3, Fig. 6). Thus no effect was detected from the U1 gene knockout in vegetatively growing cells other than the growth rate limitation due to the reduction in total H3 synthesis. The similar effect was seen in U2KO strains where cell doubling rates were increased more than two-fold (Fig. 6H) when the major source of H3 protein, RC H3.2, was deleted. In Tetrahymena a similar reduction in growth rate was observed in RC H3 knockouts, although this effect could be partially compensated for by upregulation of a RI H3 locus (9). Such an effect

on U1 expression in U2KO strains was not detected in Ustilago. In stationary cultures, the only difference observed between wt and knockout strains was an earlier browning (i.e. dying) of the KO cells. However, contrary to the expectation based on the synthesis and incorporation of H3 variant proteins in stationary cells (Fig. 6D), this effect was stronger for U2KO cells where H3.1 incorporation continued, than for U1KO strains where no histone H3 protein was incorporated into the chromatin of non-proliferating cells (lane U1KO-Stat in Fig. 6D). Nucleosomal density differences in the chromatin of these knockout strains are being investigated in an attempt to identify the basis for this effect.

REFERENCES

1. Urban, M. K., and Zweidler, A. (1983) *Dev. Biol.* **95**, 421-428
2. Ridsdale, J. A., and Davie, J. R. (1987) *Nucleic Acids Res.* **15**, 1081-1096
3. Lewis, P. W., Elsaesser, S. J., Noh, K. M., Stadler, S. C., and Allis, C. D. (2010) *Proc. Natl. Acad. Sci. U. S. A.* **107**, 14075-14080
4. Elsaesser, S. J., Goldberg, A. D., and Allis, C. D. (2010) *Curr. Opin. Genet. Dev.* **20**, 110-117
5. Takayama, Y., and Takahashi, K. (2007) *Nucleic Acids Res* **35**, 3223-3237
6. Waterborg, J. H. (2011) *Biochem. Cell Biol.* **In Press**
7. Thatcher, T. H., MacGaffey, J., Bowen, J., Horowitz, S., Shapiro, D. L., and Gorovsky, M. A. (1994) *Nucleic Acids Res.* **22**, 180-186
8. Waterborg, J. H., and Robertson, A. J. (1996) *J. Mol. Evol.* **43**, 194-206
9. Cui, B., Liu, Y., and Gorovsky, M. A. (2006) *Mol. Cell. Biol.* **26**, 7719-7730
10. Ahmad, K., and Henikoff, S. (2002) *Mol. Cell* **9**, 1191-1200
11. Kamper, J., Kahmann, R., Bolker, M., Ma, L. J., Brefort, T., Saville, B. J., Banuett, F., Kronstad, J. W., Gold, S. E., Muller, O., Perlin, M. H., Wosten, H. A., de Vries, R., Ruiz-Herrera, J., Reynaga-Pena, C. G., Snetselaar, K., McCann, M., Perez-Martin, J., Feldbrugge, M., Basse, C. W., Steinberg, G., Ibeas, J. I., Holloman, W., Guzman, P., Farman, M., Stajich, J. E., Sentandreu, R., Gonzalez-Prieto, J. M., Kennell, J. C., Molina, L., Schirawski, J., Mendoza-Mendoza, A., Greilinger, D., Munch, K., Rossel, N., Scherer, M., Vranes, M., Ladendorf, O., Vincon, V., Fuchs, U., Sandrock, B., Meng, S., Ho, E. C., Cahill, M. J., Boyce, K. J., Klose, J., Klosterman, S. J., Deelstra, H. J., Ortiz-Castellanos, L., Li, W., Sanchez-Alonso, P., Schreier, P. H., Hauser-Hahn, I., Vaupel, M., Koopmann, E., Friedrich, G., Voss, H., Schluter, T., Margolis, J., Platt, D., Swimmer, C., Gnirke, A., Chen, F., Vysotskaia, V., Mannhaupt, G., Guldener, U., Munsterkotter, M., Haase, D., Oesterheld, M., Mewes, H. W., Mauceli, E. W., DeCaprio, D., Wade, C. M., Butler, J., Young, S., Jaffe, D. B., Calvo, S., Nusbaum, C., Galagan, J., and Birren, B. W. (2006) *Nature* **444**, 97-101
12. Brachmann, A., Konig, J., Julius, C., and Feldbrugge, M. (2004) *Mol. Genet. Genomics* **272**, 216-226
13. Garcia-Muse, T., Steinberg, G., and Perez-Martin, J. (2003) *Eukaryotic cell* **2**, 494-500
14. Waterborg, J. H. (1990) *J. Biol. Chem.* **265**, 17157-17161
15. Waterborg, J. H. (2002) Acetic acid-urea polyacrylamide gel electrophoresis of basic proteins. in *The protein protocols handbook, 2nd edition* (Walker, J. M. ed.), Humana Press, Totowa NJ. pp 103-111

16. Waterborg, J. H. (2002) Acid-urea-Triton polyacrylamide gel electrophoresis. in *The protein protocols handbook, 2nd edition* (Walker, J. M. ed.), Humana Press, Totowa NJ. pp 113-123
17. Waterborg, J. H. (1998) *J. Biol. Chem.* **273**, 27602-27609
18. Waterborg, J. H., Robertson, A. J., Tatar, D. L., Borza, C. M., and Davie, J. R. (1995) *Plant Physiol.* **109**, 393-407
19. Flor-Parra, I., Vranes, M., Kamper, J., and Perez-Martin, J. (2006) *Plant Cell* **18**, 2369-2387
20. Scherer, M., Heimel, K., Starke, V., and Kamper, J. (2006) *Plant Cell* **18**, 2388-2401
21. Tsukuda, T., Carleton, S., Fotheringham, S., and Holloman, W. K. (1988) *Mol. Cell. Biol.* **8**, 3703-3709
22. Stewart, C. N., Jr., and Via, L. E. (1993) *BioTechniques* **14**, 748-750
23. Pitkin, J. W., Panaccione, D. G., and Walton, J. D. (1996) *Microbiol* **142 (Pt 6)**, 1557-1565
24. Kojic, M., Ninghui, M., Qingwen, Z., Lisby, M., and Holloman, W. K. (2008) *Mol. Microbiol.* **67**, 1156-1168
25. Zweidler, A. (1980) *Dev. Biochem.* **15**, 47-56
26. Waterborg, J. H. (1993) *J. Biol. Chem.* **268**, 4912-4917
27. Waterborg, J. H. (1991) *Plant Physiol.* **96**, 453-458
28. Waterborg, J. H. (1992) *Plant Mol. Biol.* **18**, 181-187
29. Steinberg, G., and Perez-Martin, J. (2008) *Trends Cell Biol.* **18**, 61-67
30. Zweidler, A. (1978) *Methods Cell Biol.* **17**, 223-233
31. Ridsdale, J. A., Rattner, J. B., and Davie, J. R. (1988) *Nucleic Acids Res.* **16**, 5915-5926
32. Waterborg, J. H., and Kapros, T. (2002) *Biochem. Cell Biol.* **80**, 279-293
33. Waterborg, J. H. (2002) *Biochem. Cell Biol.* **80**, 363-378
34. Kapros, T., Robertson, A. J., and Waterborg, J. H. (1995) *Plant Mol. Biol.* **28**, 901-914
35. Holloman, W. K., Schirawski, J., and Holliday, R. (2008) *Fungal Genet. Biol.* **45 Suppl 1**, S31-39
36. Holloman, W. K., Schirawski, J., and Holliday, R. (2007) *Trends Microbiol.* **15**, 525-529
37. Ruiz-Herrera, J., Leon, C. G., Guevara-Olvera, L., and Carabez-Trejo, A. (1995) *Microbiol* **141**, 695-703
38. Waterborg, J. H. (2000) *J. Biol. Chem.* **275**, 13007-13011
39. Garcia, B. A., Hake, S. B., Diaz, R. L., Kauer, M., Morris, S. A., Recht, J., Shabanowitz, J., Mishra, N., Strahl, B. D., Allis, C. D., and Hunt, D. F. (2007) *J. Biol. Chem.* **282**, 7641-7655
40. Adkins, M. W., Carson, J. J., English, C. M., Ramey, C. J., and Tyler, J. K. (2007) *J. Biol. Chem.* **282**, 1334-1340
41. Minard, L. V., Williams, J. S., Walker, A. C., and Schultz, M. C. (2011) *J. Biol. Chem.* **286**, 7082-7092
42. Tang, Y., Holbert, M. A., Delgoshaie, N., Wurtele, H., Guillemette, B., Meeth, K., Yuan, H., Drogaris, P., Lee, E. H., Durette, C., Thibault, P., Verreault, A., Cole, P. A., and Marmorstein, R. (2011) *Struct.* **19**, 221-231
43. Aslam, A., and Logie, C. (2010) *PLoS ONE* **5**, e10851
44. Masumoto, H., Hawke, D., Kobayashi, R., and Verreault, A. (2005) *Nature* **436**, 294-298
45. Thaminy, S., Newcomb, B., Kim, J., Gatbonton, T., Foss, E., Simon, J., and Bedalov, A. (2007) *J. Biol. Chem.* **282**, 37805-37814

46. Agez, M., Chen, J., Guerois, R., van Heijenoort, C., Thuret, J. Y., Mann, C., and Ochsenbein, F. (2007) *Struct.* **15**, 191-199
47. Xhemalce, B., Miller, K. M., Driscoll, R., Masumoto, H., Jackson, S. P., Kouzarides, T., Verreault, A., and Arcangioli, B. (2007) *J. Biol. Chem.* **282**, 15040-15047
48. Luger, K., Mader, A. W., Richmond, R. K., Sargent, D. F., and Richmond, T. J. (1997) *Nature* **389**, 251-260
49. Waterborg, J. H. (1990) *Electrophoresis* **11**, 638-641

FOOTNOTES

* We gratefully thank Kevin McCluskey (Fungal Genetics Stock Center, University of Missouri, Kansas City, MO), Scott Gold (University of Georgia, Athens, GA), Michael Feldbrügge (University of Düsseldorf, Germany), and Jörg Kämper and Regine Kahmann (University of Marburg, Germany) for providing strains, plasmids, technical and scientific advice. This research was supported by the Missouri Life Sciences Research Board, award 13254 to JHW.

Abbreviations used: AcK, acetylated lysine; *AcK, tritiated acetylated lysine; AUT, acid urea Triton; bp, basepairs; KO, knockout; PCR, polymerase chain reaction; qRT, quantitative reverse transcription; RC, replication coupled; RI, replication independent.

FIGURE LEGENDS

Fig. 1. Histone H3 genes of *Ustilago maydis*. (A) structural organization of histone H3 gene U1 for histone variant H3.1 on chromosome 11 and U2 for histone variant H3.2 on chromosome 6 in a divergently transcribed pairing with the single histone H4 gene (11). Transcribed sequences are indicated by a bold line. Arrows mark start and direction of gene transcription. Intron locations in the 5' untranslated region and at codon 98 of H3.1 and at codon 15 of H3.2 are marked. A 1 kb size marker is shown. (B) Comparison of U1 and U2 protein products with positions 1-135 of the mature proteins and sequence differences marked by stars and highlighted as bolded capitals.

Fig. 2. Separation, identification and post-translational modification of H3 histones. (A) Separation of H3 variants, co-eluted from reversed-phase hplc, in an acid urea (AU) gradient gel with Triton X-100 from 0 to 10 mM where H3 variants co-electrophorese under AU conditions at 0 mM Triton. The slant in electrophoretic mobility across the gradient, marked by methylene blue at the discontinuous running front, by non-histone proteins in this partially purified hplc H3 pool and by two guidance lines, results from the glycerol gradient used to stabilize the gradient gel (16). The characteristic high affinity for Triton of core histone H3 is modulated by differences of exposed side chains within the histone fold of the H3 variants (Fig. 1B) (48,49). The broken line marks the optimal concentration of 6 mM Triton X-100 in 8 M urea and 1 M acetic acid for the separation of the H3 variants of *U. maydis*. (B) Pattern of H3 variants in AUT gels, pulse-labeled *in vivo* with [^{35}S] methionine for 20 min at 0.1 mCi/L (lanes A-B), or with [^{3}H]-lysine for 30 min at 0.4 mCi/L (lanes C-D) or chased for 24 hrs in fresh SD medium into stationary phase (lanes E-F). Coomassie-stained gel lanes are marked by 'c' and 33 day fluorographic exposures by 'f'. Non-acetylated and hexa-acetylated H3 species are marked by 0 and 6, respectively. (C) Pattern of histone H3 variants in logarithmically growing cultures, incubated with 4 mCi/L [^{3}H]-acetic acid for 5 min (lanes A-B) or 20 min (lanes C-D). Coomassie-stained gel lanes are marked by 'c' and 18 day fluorographic exposures by 'f'. Non-acetylated through hexa-acetylated H3 species are marked by 0 to 6, respectively.

Fig. 3. Changes in H3 variant abundance and steady-state acetylation. (A) Histone H3 variants were isolated from mid-log phase cultures (0.4 x 10^{7} cells/ml), marked as 0 h (log), and after 2, 6 and 12.5

hours continued culture into stationary phase (stat). (B) The increased abundance of H3.1, expressed as a percentage of total histone H3 (line), during continued growth coincides with reduced levels of histone H3 acetylation (broken line) and cessation of cell budding.

Fig. 4. Histone H3 variant genes differ in cell cycle expression patterns. (A) Histone H3 proteins, labeled at 0.5 h intervals after release from treatment with hydroxyurea (1 mg/ml) for 0.5 h with tritiated lysine, eluted between 41 and 46 min after hplc column loading (see Experimental Procedures) as determined by absorbance (Abs.) at 214 nm. The presence of lysine label was determined in each 1 ml fraction (cpm/fr) by liquid scintillation counting. Based on lysine labeling, peaks in histone H3 synthesis rates were observed in samples labeled from 0.5 to 1.0 h and from 2.5 to 3.0 h after release from the hydroxyurea block. The time after release shown is the time that cells were collected for histone purification. (B) Pooled histone H3 preparations collected at 0.5 h intervals after lysine labeling for 0.5 h were separated by AUT gel electrophoresis and stained with Coomassie. The relative amounts of the H3.1 and H3.2 proteins, and the amounts of all acetylated species (non- through hexa-acetylated species are marked) were determined by densitometry. Radioactivity in all bands was quantitated by densitometry of fluorographs exposed for varying length of time (a 30-day exposure is shown in panel C) and the calculated specific radioactivity is shown in panel E. (D) The cell density in cultures released from hydroxyurea was determined by hemocytometer counting (broken line). The biphasic histone H3 hplc elution pattern, which was most prominent at 1 and 3 hrs after release from hydroxyurea, was shown to consist of a late-eluting form of newly synthesized histone H3 and an early-eluting bulk form of histone H3 (See Fig. 5). The relative amount of late-eluting, new H3, to the right of the line in each of the graphs of panel A, is shown by the continuous line, expressed as a percentage of total H3 protein. The gray bar represents hydroxyurea treatment (from –90 min to 0 min). (E) Specific radioactivity in histone H3.1 (solid triangles) and H3.2 (open triangles), calculated from densitometry of the data in panel B and C, is plotted at the mid-point of the 30 min pulse labeling period. (F) The amounts of mRNA transcripts from H3.1 U1 (solid triangles), from H3.2 U2 (open triangles), and from H4 genes (open squares) was determined by qRT-PCR relative to constitutive PPI gene transcript levels. (G) FACS cell cycle analysis of samples after release from the hydroxyurea block, scored by ModFit LT. The three populations scored were, from left to right in each panel, cells in G1 phase (dark area), cells during replication (light area) and cells in G2/M phase (dark area).

Fig. 5. Histone H3 turnover identifies the H3.1 variant as a replacement histone. (A) Logarithmically growing cultures (0.5 L) at 10^7 cells/ml were incubated for 15 min with 0.1 mCi tritiated lysine, collected and chased in SD medium supplemented with 100 mg/ml lysine. Examples of the hplc absorbance at 214 nm and cpm per 0.5 ml fraction are shown after pulse labeling (0 min) and after 30, 66 and 115 min chase. Pooled fractions for main H3 (m) and new H3 (n) were fractionated by AUT gel electrophoresis, Coomassie stained (panel B) and fluorographed for 28 days (panel C). The chase time (min) for all samples is shown between panels B and C. The H3.1 and H3.2 variants are marked at non- (0) up to hexa-acetylated (6) species. (D) The relative specific radioactivity of nH3 (line with solid triangles) and mH3 (broken line with open squares) in hplc chromatography is shown as the percentage of cpm/absorbance after pulse labeling. The overall decrease in total H3 specific radioactivity (gray circles) below the initial pulse label level (dotted line) is shown with a linear fitted line. The relative specific radioactivity of H3.1 (E) and H3.2 (F) variants, calculated from fluorography (28 days) and Coomassie densitometry in panels C and B, respectively, was standardized at the start of the chase period when 38 ± 10 % (n=8) of the label is located in H3.1 (panel C, 0 min lanes). Plotted as in panel D, the linear fitted line demonstrates approximately 50 % turnover of new histone H3.1 during a 150 min chase (E) and the absence of detectable turnover of new histone H3.2 (F). In combination these effects produce the same H3.1 abundance that is seen as the Coomassie stained steady-state condition where 26 ± 1 % (n=8) of histone H3 exists as H3.1 protein (panel B).

Fig. 6. Histone H3 variant synthesis in wild-type, U1KO and U2KO cultures. (A) Histone H3 proteins extracted from wt cells, labeled for 15 min with tritiated lysine (0.3 mCi/L) during log culture (Log) at 1.5 x 10^7 cells/ml, after 6 h continued culture at 1 mg/ml hydroxyurea (HU) and after 24 h continued culture into stationary phase (Stat), were fractionated by hplc into main (m) and new (n) pools (See Fig. 5) and analyzed by AUT gel electrophoresis, stained with Coomassie (Coom.) and fluorographed for various length of time. Panel B shows a 6 day exposure for Log and a 35 day exposure for HU and Stat samples. Non-acetylated (0) through hexa-acetylated (6) forms of H3.1 and H3.2 are marked. (C) Cultures (0.8 L) of U2KO isolate 96 (U2KO), wt and U1KO isolate 47 (U1KO) cells were labeled for 30 min with 0.2 mCi/L tritiated lysine during logarithmic growth (Log) and continued growth into stationary phase (Stat) at the time and culture densities marked by stars in panels G, E and F, respectively. Histone H3 variants, separated in AUT gels, were stained with Coomassie (panel C) and fluorographed. The example of an 11 day fluorography is shown in panel D. Non-acetylated (0) through hexa-acetylated (6) forms of H3.1 and H3.2 are marked. Note that H3 yields from long-term stationary cultures of wt, U1KO and U2KO were reduced on a per cell basis to 62 ± 6 % (n=6) for all strains, likely due to cell wall thickening and the resulting decreased efficiency of cell breakage by sonication. (E) Cell density, measured by hemocytometer, of wt cells, with sub-culturing and dilution with SD medium marked by broken lines. Stars mark Log and Stat lysine labeling times and cell densities. Total cell amounts were plotted in panel H, marked by 'wt'. (F) Like E for U1KO isolate 47. (G) Like E for U2KO isolate 96. (H) Total increase in cell numbers calculated from panels E, F and G for wt, U1KO and U2KO strains. Cell doubling times calculated from exponential curve fitting (Sigmaplot) are shown.

TABLES

Table I. PCR primers.

Primer name	Primer sequence	PCR [1]
U1F	AGCGTCTCGTTCGTGAGATT	344 (235)
U1R	CGTTAGAGGCAAATGTGGAGT	
U2F	TCCAACACATAACTTCTCACTCG	292 (175)
U2R	AGGCTTCTTGACACCACCAG	
H4F	AAAGGCGGCAAGGGTCTCG	362 (260)
H4R	TTGAGTGCGTAAACAACGTCGAGC	
ppiF	TTCCCAAGACTGCCAAGAAC	267 (267)
ppiR	CGACGGTGGTGATGAAGAAC	
U1KOLBF	TCGATGAGCTCCCTGTTCGCTACCCTCTCT	863
U1KOLBR	TGGTGGCCATCTAGGCCAGGGTGTTGGAACG	
U1KORBF	ATAGGCCTGAGTGGCCTCGTCTCTCTTTCGCAT	1043
U1KORBR	AGTCTGAATTCCACCGATCCTCCTATACCA	
U2KOLBF	TCAGAGTCGACCGCACTTATCGTGCTAGTCC	1020
U2KOLBR	TGGTGGCCATCTAGGCCAGAAGCCGAATGAGCAGTGT	
U2KORBF	ATAGGCCTGAGTGGCCTATAGTGGGCGTCTGAATC	1015
U2KORBR	AGTCTAAGCTTTCCTTGTTCACCGCTCGT	

[1] PCR product in bp from DNA templates and, in brackets, from RNA/cDNA templates.

FIGURES

Figure 1.

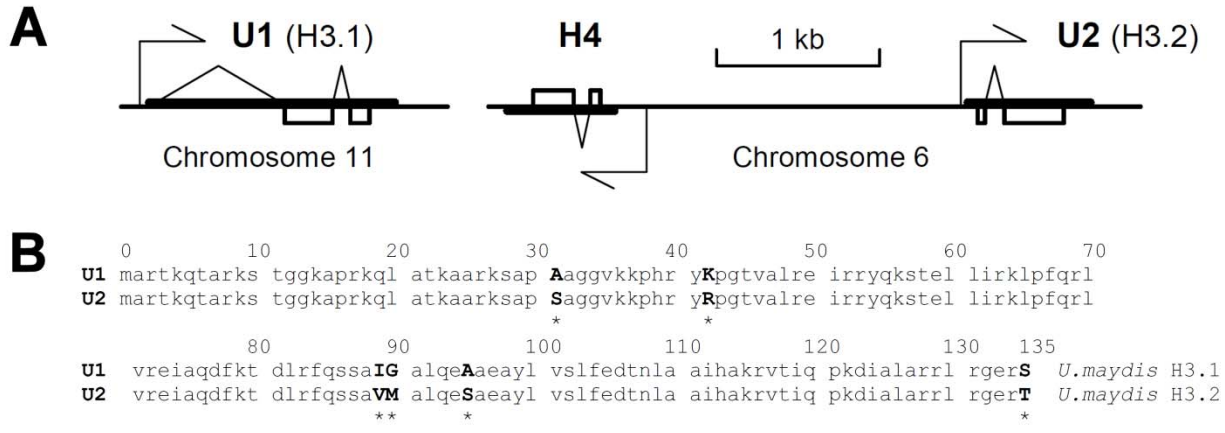

Figure 2.

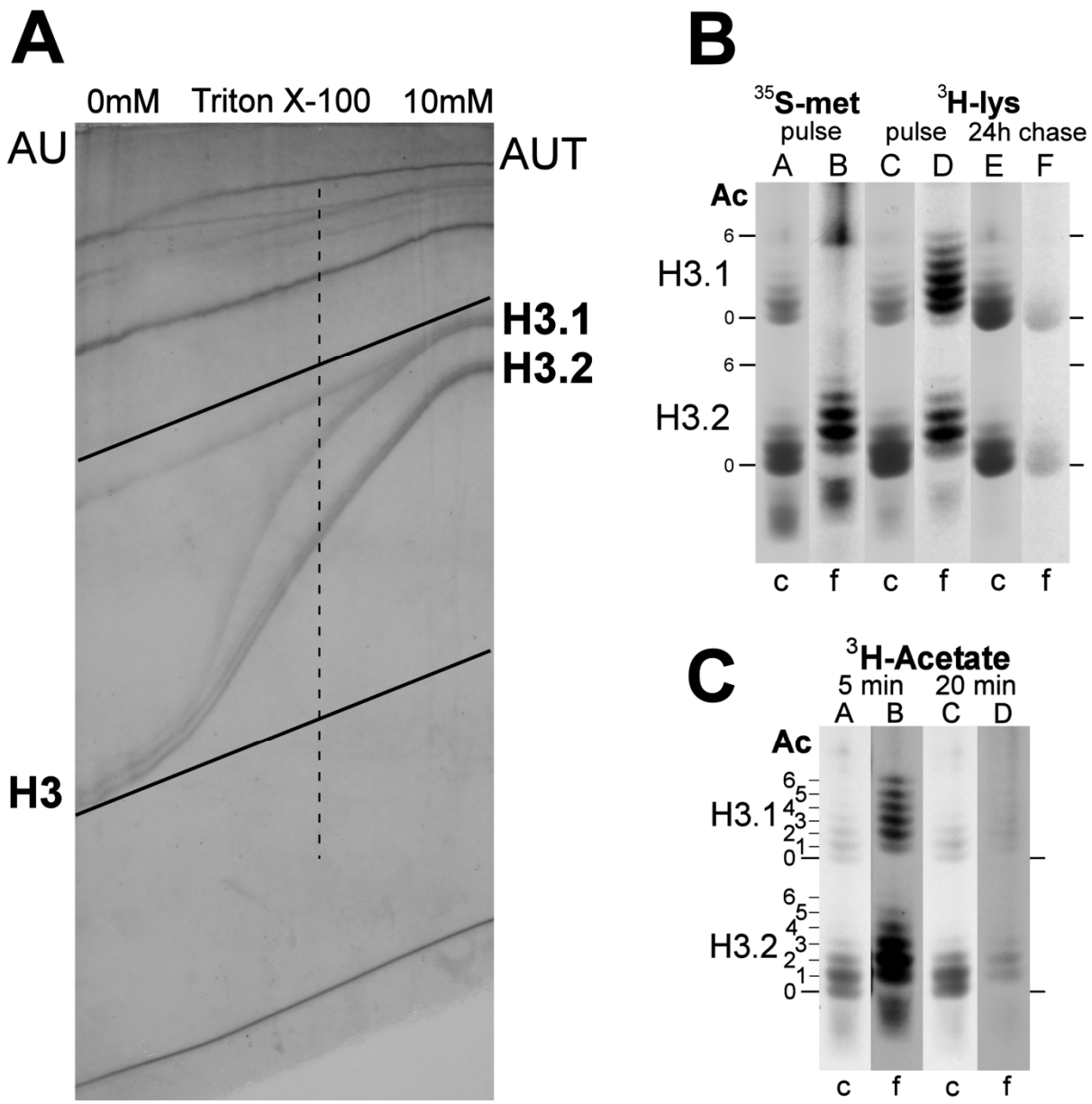

Figure 3.

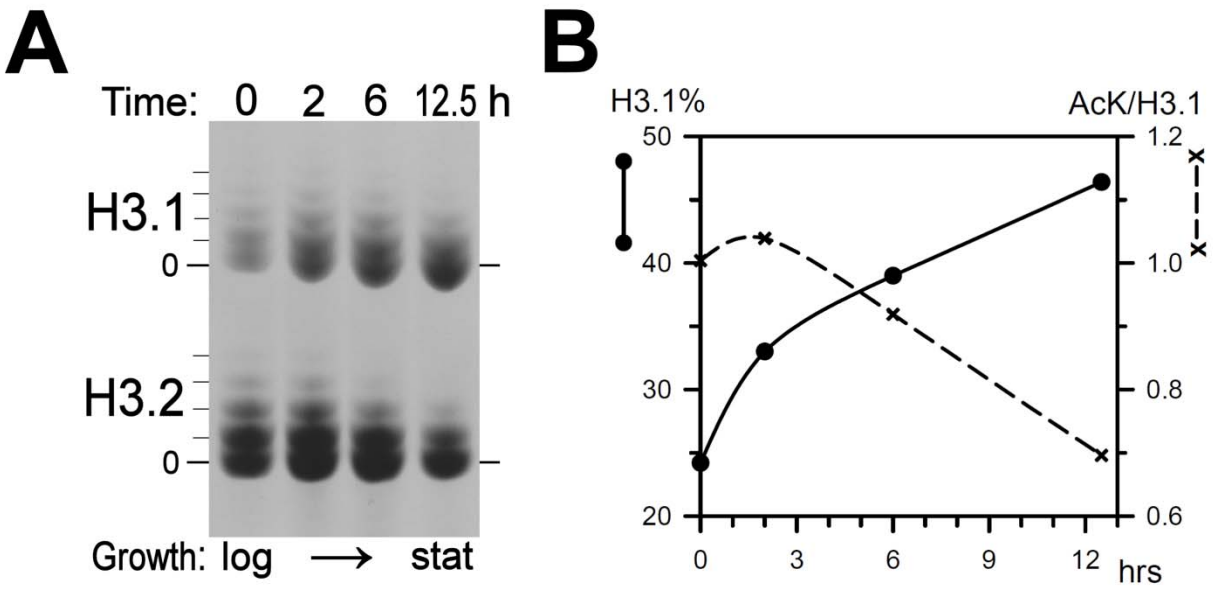

Figure 4.

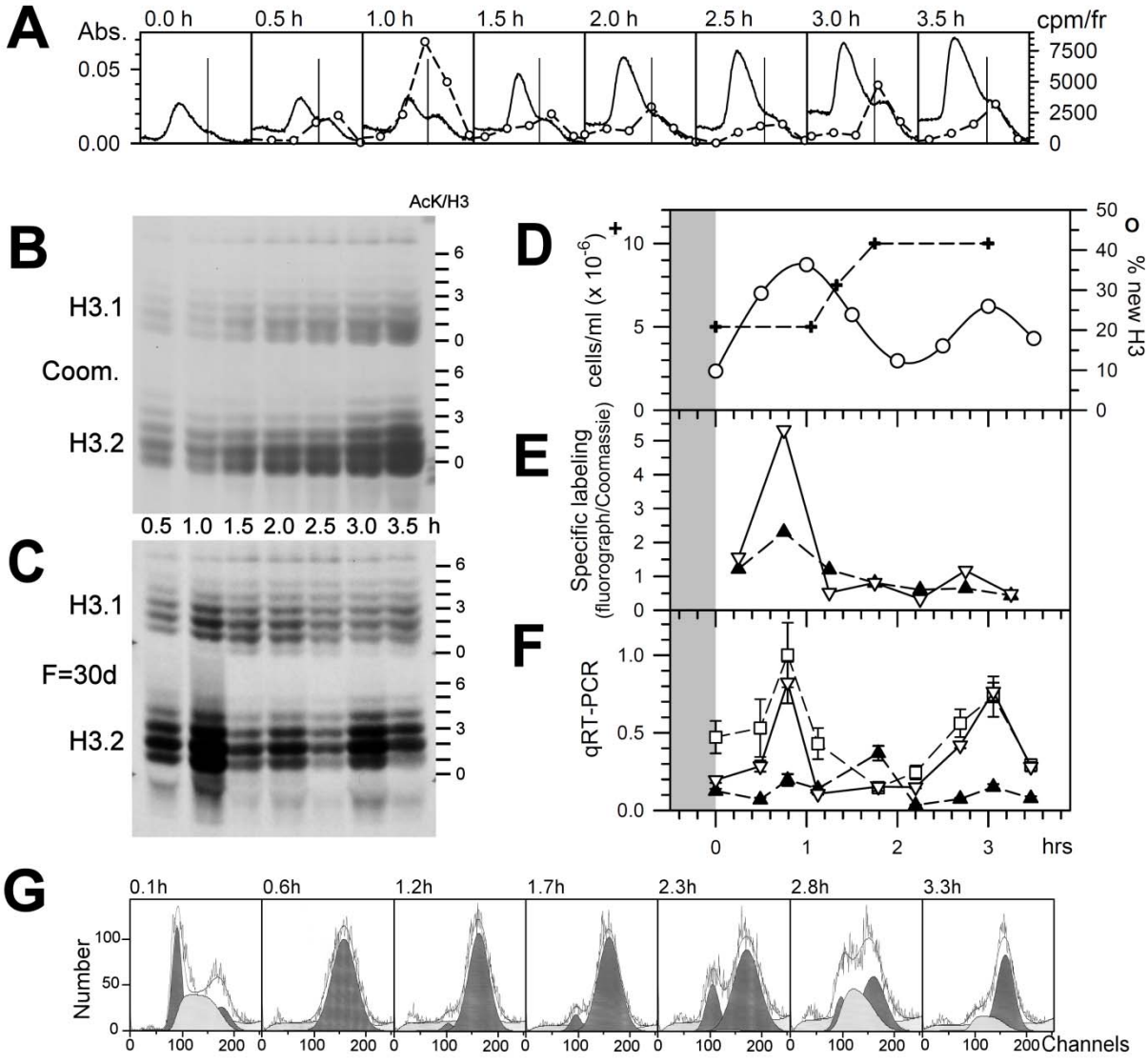

Figure 5.

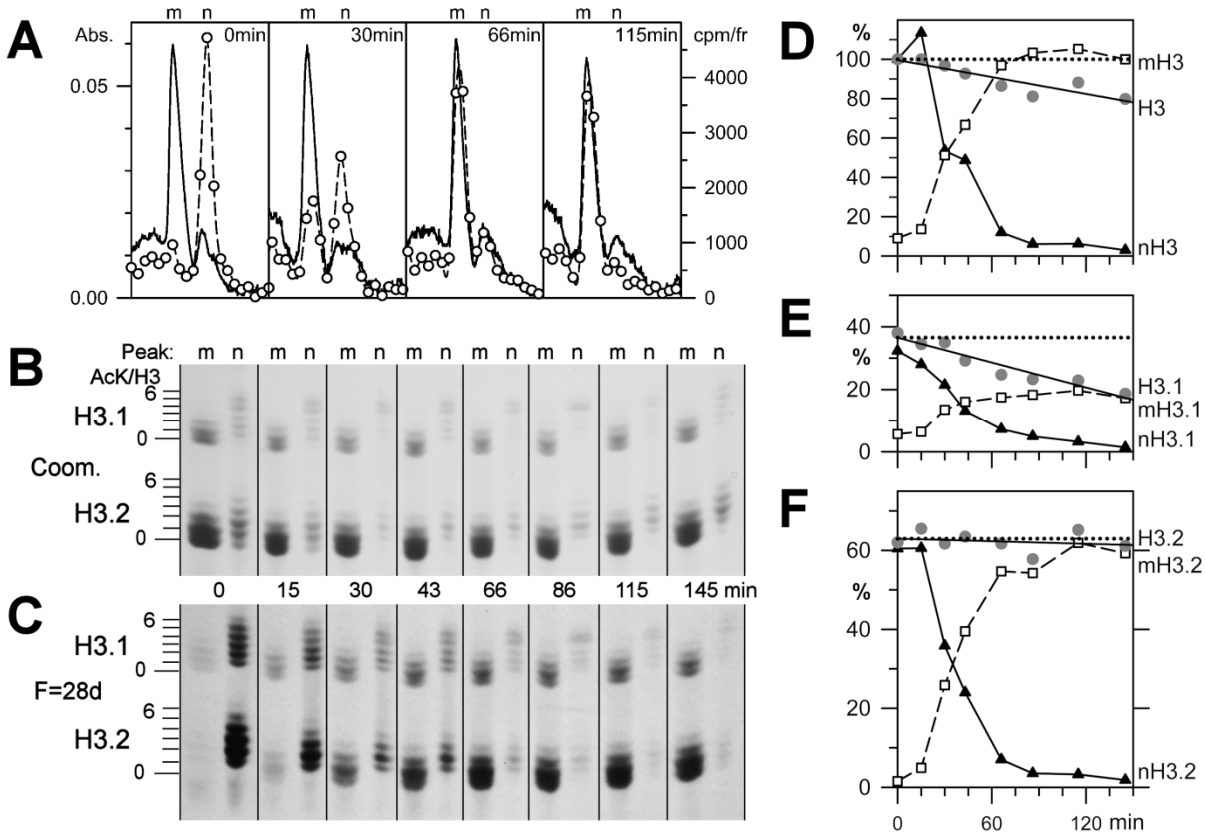

Figure 6.